Title

The stay-green phenotype of TaNAM-RNAi wheat plants is associated with maintenance of chloroplast structure and high enzymatic antioxidant activity.

Authors

Checovich, Mariana L
Galatro, Andrea
Moriconi, Jorge I
et al.

Publication Date

2016-07-01

DOI

10.1016/j.plaphy.2016.03.035

Peer reviewed

The stay-green phenotype of *TaNAM*-RNAi wheat plants is associated with maintenance of chloroplast structure and high enzymatic antioxidant activity

Mariana L. Checovich[a], Andrea Galatro[c], Jorge I. Moriconi[a], Marcela Simontacchi[b], Jorge Dubcovsky[d] and Guillermo E. Santa-María[a]*

[a] Instituto Tecnológico Chascomús (IIB-INTECH), Consejo Nacional de Investigaciones Científicas y Técnicas (CONICET) and Universidad Nacional de San Martín (UNSAM). Av. Intendente Marino km 8.2. Chascomús. Buenos Aires, 7130. Argentina.

[b] Instituto de Fisiología Vegetal (INFIVE), Universidad Nacional de La Plata (UNLP) and Consejo Nacional de Investigaciones Científicas y Técnicas (CONICET), Diagonal 113 y 61, La Plata, Buenos Aires, 1900, Argentina.

[c] Physical Chemistry-Institute of Biochemistry and Molecular Medicine (IBIMOL), School of Pharmacy and Biochemistry, University of Buenos Aires-CONICET, Junín 956, Buenos Aires, C1113AAD, Argentina.

[d] Department of Plant Sciences, One Shields Avenue. University of California, Davis, California, 95616-8515, USA.

* Corresponding author.

Dr. Guillermo E. Santa-María

Instituto Tecnológico Chascomús, Av. Intendente Marino km 8.2, Chascomús, Provincia de Buenos Aires, 7130, Argentina.

Tel.: 54 (2241) 424045

Fax: 54 (2241) 424048

email: gsantama@intech.gov.ar

Summary

TaNAM transcription factors play an important role in controlling senescence, which in turn, influences the delivery of nitrogen, iron and other elements to the grain of wheat (*Triticum aestivum*) plants, thus contributing to grain nutritional value. While lack or diminished expression of *TaNAMs* determines a stay-green phenotype, the precise effect of these factors on chloroplast structure has not been studied. In this work we focused on the events undergone by chloroplasts in two wheat lines having either control or diminished *TaNAM* expression due to RNA interference (RNAi). It was found that in RNAi plants maintenance of chlorophyll levels and maximal photochemical efficiency of photosystem II were associated with lack of chloroplast dismantling. Flow cytometer studies and electron microscope analysis showed that RNAi plants conserved organelle ultrastructure and complexity. It was also found that senescence in control plants was accompanied by a low leaf enzymatic antioxidant activity. Lack of chloroplast dismantling in RNAi plants was associated with maintenance of protein and iron concentration in the flag leaf, the opposite being observed in control plants. These data provide a structural basis for the observation that down regulation of *TaNAM*s confers a functional stay-green phenotype and indicate that the low export of iron and nitrogen from the flag leaf of these plants is concomitant, within the developmental window studied, with lack of chloroplast degradation and high enzymatic antioxidant activity.

Highlights

•*TaNAM*-RNAi stay-green phenotype is coupled with maintenance of chloroplast structure.
•That stay-green phenotype is associated with a high enzymatic antioxidant activity.
•Chloroplast dismantling correlates with decay of iron and protein content in leaves.

Keywords
Chloroplast, NAM, senescence, stay-green, *Triticum aestivum*, wheat

Abbreviations

AA, After anthesis
APX, Ascorbate peroxidase (**EC 1.11.1.11**)
DAA, Days after anthesis
EDTA, Ethylene diamine tetracetic acid
HEPES, (N-[2-Hydroxyethyl]piperazine-N'-[2-ethanesulfonic acid])
SOD, Superoxide dismutase (**EC 1.15.1.1)**

RNAi, RNA interference
ROS, reactive oxygen species

1. Introduction

In cereal crops the extension of the period that leaves remain green has been frequently proposed as a desirable trait to extend the period of grain filling, which might impact positively on yield. For the particular case of wheat this view has been partially questioned as the grain filling capacity instead of the capacity to maintain an adequate supply of photosynthates could be, at least in some circumstances, the limiting step in determining the grain mass. Thus, it has been proposed that a tandem increase of grain filling and residual photosynthesis capacities could lead to increased yield (Borrill et al., 2015). On the other hand, it has been also noted that maintenance of the stay-green trait can be reached through multiple ways, and only in some of them disabling of the photosynthetic machinery could be delayed (Thomas and Howart, 2000). Therefore, the purpose to increase wheat yield through the use of stay-green mutants likely would require an integrated approach as well as in-depth knowledge on the precise role of each mutation on the stay-green trait. Stay-green mutants have been broadly classified into two groups: cosmetic and functional. Functional stay-green mutants are those in which both photosynthesis and chlorophyll degradation are delayed relative to "normal" plants (Thomas and Ougham, 2014). On the contrary, in cosmetic stay-green plants chlorophyll catabolism is compromised while photosynthesis progressively decays. Characterization of stay-green mutants has been mainly done through an examination of the correspondence between the patterns of chlorophyll accumulation and photosynthesis. While several stay-green wheat mutants have been identified, detailed studies on the chloroplast structural properties and biochemical pathways coupled with this trait remain scant. Nevertheless, some advances have been achieved. In this regard, it has been recently proposed that regeneration of chloroplast structure is a key component in the difference between a functional stay-green accession and an agronomic parental line (Luo et al., 2013). Furthermore a detailed study on the chloroplast structure of wheat plants just differing in a specific mutation determining a stay-green phenotype has recently been performed for the *tsga1* mutant (Tian et al., 2012). On the other hand, whilst the involvement of reactive oxygen species (ROS) during plant senescence either as determinants of cell injury as well as in the signalling network has

been widely documented (Thompson et al., 1987; Prochazkova et al., 2001; Krieger-Liszkay et al., 2015), only recently a possible link between the way that wheat plants handle ROS accumulation and the stay-green trait started to emerge (Hui et al., 2012; De Simone et al., 2014).

An additional important challenge in wheat production is to improve the nutritional quality of the grains in terms of protein content and the concentration of some specific nutrients such as iron and zinc (Cakmak et al., 2004; Kade et al., 2005). Early efforts in this crop uncovered the existence of a high grain protein content (GPC) trait derived from a wild emmer wheat accession located in the short arm of chromosome 6B (Joppa et al., 1997). The corresponding allele, when introgressed into modern hexaploid wheat cultivars, leads to enhanced protein content which in some cases has been accompanied by detrimental effects on grain size (Brevis and Dubcovsky 2010; Tabbita et al., 2013). With the exception of some spring swedish varieties which possess a rare allele of GPC (Asplund et al., 2013), most modern *Triticum aestivum* cultivars do not possess a functional version due to a frame shift mutation in the coding region of the gene (Uauy et al., 2006). Positional cloning of the wild emmer wheat gene determining this trait revealed that it belongs to the NAC family of transcription factors, thereafter named as *TtNAM-B1* (Uauy et al., 2006). That study also unveiled that several homologous of *TaNAM* are present in the hexaploid wheat genome, and an RNA interference (RNAi) based procedure was used to reduce the level of expression of all those copies. The resulting RNAi plants display a pronounced delay in the decay of chlorophyll content. Although the original identification took place in wheat plants, it was next shown that in barley, a species closely related to wheat, homologous genes also contribute to accelerated senescence (Distelfeld et al., 2008; Jukanti et al. 2008; Jamar et al., 2010; Cai et al., 2013). Interestingly, identification and characterization of the closest homologue in rice suggested that conservation of the functional role is in fact restricted to some Poaceae groups indicating a dynamic history of NAC transcription factors in grasses (Distelfeld et al., 2012). In *Arabidopsis thaliana* it has been established that some NAC transcription factors could modulate senescence by controlling chloroplast maintenance (Garapati et al. 2015). In spite of the obvious interest of the stay-green phenotype derived from diminished NAM expression in Triticeae, no

studies have compared the chloroplast ultra-structure and the biochemical changes suffered by flag leaves of *TaNAM* and *TaNAM*-RNAi plants.

A recent study showed that mutations that specifically led to lack of function of the *TaNAM-B1* homeologous genes *TaNAM-A1* and *TaNAM-D1* also led to an stay-green phenotype; which has been characterized as a functional one (Avni et al., 2014). Further studies with *TaNAM*-RNAi lines led to a similar conclusion (Borrill et al., 2015). It has been thought that the reduced delivery of nitrogen, iron and zinc from the leaves of *TaNAM*-RNAi plants is determined, at least partially, by preservation of chloroplast structure reducing the amount of nutrients available for long-distance export (Distelfeld et al., 2007; Waters et al., 2009). Although reasonable, up to date no direct evidence supporting this hypothesis has been provided. In this context, the aim of this work was to study to which extent the stay-green phenotype of *TaNAM*-RNAi plants is actually concomitant with lack of chloroplast dismantling and to explore biochemical changes that accompanied the action of TaNAM transcription factors.

2. Materials and methods

2.1 Plant material and growth conditions

Two *Triticum aestivum* cv Bobwhite lines were used in this work. In one of them, hereafter named as RNAi line, RNAi was used to reduce expression of all *TaNAM* coding genes, while the second one was a control line which displays "normal" expression levels of *TaNAM* genes (Uauy et al., 2006). A homozygous RNAi-positive line and a homozygous RNAi-negative (T3) line were used for the experiments. The presence or absence of the transgene was checked by PCR through the use of specific PCR markers as described by Uauy et al (2006). Seeds were surface sterilized with bleach (5% v/v) for 5 min and were then washed with pure water and germinated in the dark on filter paper imbibed with deionized water. On day five after sowing, the seedlings were transferred to the plant growth facility and placed in a 5 L pot filled with a mix of sand and silt loam soil (1:3 v/v). To this mix a fertilizer containing N, P and K (15, 6, 12 %) was previously added at a rate

of 0.5 g/L. Pots were watered as necessary. Two experiments were made, in one of them transference of seedlings took place on March 13th, 2013 and in the other on August 14th 2013. Except were indicated any further reference corresponds to plants transferred on August 14th.

Plants reached fifty percent anthesis, as determined by anther opening in the spike of the main axis, on day 65 after sowing. No differences in the time to anthesis were detected between lines. On that day, the flag leaf of individual plants was labelled. Two harvests were made, the first one took place when no symptoms of senescence, as determined by measuring the SPAD index, were evident in any of the two lines used. The second one was performed soon after consistent differences in the SPAD index between lines were observed. The first harvest was performed on day 14 after anthesis (here after AA); while the second one was made on day 24 AA.

2.2 Measurement of SPAD index and maximal photochemical efficiency of photosystem II

For the flag leaf of individual plants, SPAD index and chlorophyll fluorescence were recorded periodically. SPAD index was measured in the flag leaf of 20 independently grown plants of each genotype through the use of SPAD-502, Minolta, Milton Keynes UK. In each leaf, 10 measurements covering the entire leaf blade were recorded, and the mean value was considered as a representative measurement of the whole leaf blade.

In order to estimate the maximum quantum yield of photosystem II, the portable fluorometer Pocket PEA Hansatech® was employed. In this case, the clip was placed in the middle zone of the leaf blade which was kept in darkness for 20 min. Subsequently the clip was opened and the leaf region exposed for 30 sec to a 3500 μmol m^{-2} s^{-1} photon flux density (peak at 637 nm). The Pocket PEA (PEA plus v1.1, Hansatech Instrument Ltd., UK) software was used to derive the maximal photochemical efficiency of photosystem II (Fv/Fm).

2.3 Determination of iron concentration in the samples

The blades of flag leaves of 15 independently grown plants of each genotype were harvested. Immediately after separation from the plant, leaves were conserved at -80°C. Leaves were powdered in liquid nitrogen, dried and weighted. In order to determine iron concentration, samples were reduced to ashes in a muffle furnace at 550°C during an 8 h period. Ashes were suspended in 0.5 mL HNO_3 65% and diluted with pure water until to reach a final volume of 3.5 mL. Determination of iron in the samples was made through the use of an atomic absorption spectrophotometer AAnalyst 100 (Perkin Elmer).

2.4 Protein concentration and SDS-PAGE

Fifteen flag leaves, taken each one of them from independently grown plants per genotype were harvested, exposed to liquid nitrogen, and immediately stored at -80 °C. Leaves were clustered into 5 groups (three flag leaves per group). Each one of these groups was considered as a replicate. The collected material, was subsequently ground in the presence of liquid nitrogen. The powdered material was used for the following biochemical determinations: protein, carbohydrates and thiols content, protein carbonylation and antioxidant enzymes activity.

To 300 mg of powdered leaves, 450 µL of extraction buffer composed of Tris-HCl 50 mM (pH 7), $MgCl_2$ 3 mM, EDTA 1 mM and polyvinylpolypyrrolidone 1% (w/v) were added. Samples were centrifuged at 4°C for 20 min at 10000 *g*. The content of proteins in the supernatant was determined through the method of Bradford (1976) and referred to the weight of the tissue. Additionally, the profile of proteins was studied by performing electrophoresis using the above extracts. For this aim, the homogenates were incubated in 0.04 M Tris-HCl pH 6.8 containing SDS 1 % (w/v), β-mercaptoethanol 2 % (v/v), glycerol 10% (v/v), and bromophenol blue 0.005 % (w/v) for 10 min at 100°C, and were separated by electrophoresis in 14% SDS-polyacrylamide gels. In each lane a sample, corresponding to 6.5 mg of fresh tissue , was loaded. Staining was made with Coomassie Brilliant Blue R-250 (BioRad).

2.5 Determination of soluble and non-soluble carbohydrates

In order to determine soluble and non-soluble carbohydrates, a sample of each one of the groups above mentioned was used. Ten mg of frozen material was mixed with 250 µL ethanol 80% and incubated at 80°C for 20 min, and subsequently centrifuged at 16000 *g* for 5 min. The supernatant was collected, and this step repeated three times. Soluble carbohydrates were determined in the ethanol extract. On the other hand, the pellet was treated with 900 µL HCl 3% (v/v), placed in a block at 110°C for 2 h, and then filtered and used to determine non-soluble carbohydrates. Determination of carbohydrates in the ethanol extract and the treated pellet was performed through the phenol-sulfuric method (Dubois et al., 1956). Additionally, sucrose, glucose and fructose were measured by an enzymatic method in the ethanol extract (Dominguez et al. 2013).

2.6 Carbonyl content in proteins

The powdered samples were homogenized with 100 mM phosphate buffer, pH 7.0 and centrifuged at 10000 g for 20 min. The supernatant was used for determination of protein oxidation. Carbonyl groups were derivatized by reaction with 2,4-dinitrophenylhidrazine as described by Levine et al (1994). After 1 h at room temperature, proteins were precipitated with trichloroacetic acid (10 % w/v final concentration). After exhaustive washing with ethanol:ethyl acetate (1:1), pellets were resuspended in 6M guanidine. The absorbance was measured at 360-390 nm (ε=22000 M^{-1} cm^{-1}), and carbonyl content in each sample expressed in relation to total soluble protein content.

2.7 Total thiol content

The powdered leaves were homogenised in the presence of tricloroacetic acid 3% (w/v final concentration), and centrifuged at 3000 *g* for 20 min. The supernatant was diluted with potassium phosphate buffer 100 mM, EDTA 5 mM pH 7.5. Total thiol content was determined at 412 nm after reduction of 5,5'-ditiobis-(2-nitrobenzoic acid) (Sies and Akerboom, 1984).

2.8 Enzyme assays

Homogenates were prepared as described in *2.4*. Total superoxide dismutase (SOD, **EC 1.15.1.1**) activity was determined spectrophotometrically in the supernatant by measuring the inhibition of xanthine oxidase dependent reduction of nitroblue tetrazolium at 560 nm. Ascorbate peroxidase (APX, **EC 1.11.1.11**) activity was assessed by following the consumption of ascorbate in the presence of hydrogen peroxide (λ 290 nm). For a detailed description of the methods used for both enzyme assays see Moriconi et al (2012).

2.9 Chloroplast isolation and flow cytometry analysis

Chloroplast isolation was made on days 14 and 24 AA according to Jasid et al (2006). In order to obtain a representative sample of plant population, flag leaves of 10 independently grown plants were grouped, and each group was considered a replicate. Four groups were created for each genotype. Leaves of each group maintained at 4^{o}C were immediately cut with a blade scissor, and subsequently homogenised with a hand blender (Braun MR-300), employing short periods of blending (1 or 2 seconds), in the isolation buffer containing 50 mM HEPES, pH 7.6, 330 mM sorbitol, 2 mM EDTA, 1 mM $MgCl_2$, 0.05% (w/v) bovine serum albumin, 5 mM ascorbic acid, and protease inhibitors (0.2 mM phenylmethylsulfonyl fluoride (PMSF), 10 μM leupeptin, 1 μM aprotinin). The ascorbic acid, PMSF, leupeptin and aprotinin were added to the buffer just before the homogenization procedure. The homogenate was filtered through two layers of Miracloth and centrifuged during 7 min at 1500 *g* at 4°C. The supernatant was discarded, and the pellet was gently suspended in 1 mL of homogenization buffer. The resuspended pellet was placed onto 10 mL of Percoll cushion (50 mM HEPES, pH 8.0, 330 mM sorbitol, 30% [v/v] Percoll) and centrifuged at 5000 *g* for 12 min. The pellet was suspended in 1 ml of resuspension buffer (50 mM HEPES, pH 8.0, 330 mM sorbitol) and centrifuged at 1500 *g* for 5 min at 4°C. The washing procedure was repeated twice and the final pellet was resuspended in 600 μl of the same buffer. In order to obtain a quantitative assessment of relevant chloroplast properties 10 μl of this sample were taken for flow cytometry analyses by using a Becton-Dickinson FACS Calibur flow cytometer equipped with standard 15 mW blue argon-ion laser (488 nm emission). Chloroplast were identified by plotting the FL3

(red fluorescence after blue light excitation) vs FSC (forward scatter). A region with appropriate size and fluorescence associated to chlorophyll was recognized. The size of each member of this population was estimated through the forward scatter, while granularity was estimated through the side scatter. In order to confirm that this population actually corresponds to chloroplasts, in preliminary runs it was sorted and subsequently observed with a fluorescence microscope.

2.10 Transmission electronic microscopy

Before and after senescence symptoms became evident, flag leaves of three independent plants were harvested. The middle zone of the leaf blade was sectioned with a razor blade into 2 mm^2 patches, which were then treated with glutaraldehyde 2% dissolved in phosphate buffer (pH 7.2-7.4) for 2 h at 4ºC. Secondary fixation was performed with OsO_4 1% for 1 h at 4ºC. Samples were carefully dehydrated by progressive treatment with ethanol and later embedded in Spurr resin (Ted Pella Inc.). Sections were stained with uranyl acetate and lead citrate, and examined with the transmission electron microscope JEM 1200 EX II (JEOL Ltd., Tokio, Japan). Pictures were taken with an Erlangshen ES1000W camera 785 (Gatan Inc., Pleasanton, California, USA).

2.11 Statistical analyses

Statistical analyses of the data were carried out through the use of the InfoStat version 2014 program (FCA, Universidad Nacional de Córdoba, Argentina; http://www.infostat.com.ar). Values obtained for both genotypes at a given harvest were compared through the t-test.

3. Results

3.1 Senescence and accumulation of proteins, iron, soluble and non-soluble carbohydrates in the flag leaf of control and RNAi plants

It has previously been shown that the flag leaf of RNAi plants, down-regulated for the *TaNAM* genes of *T. aestivum,* displays a delayed senescence relative to control plants, as revealed by measurements of chlorophyll content, and also that differences between control and RNAi lines take some time to develop (Uauy et al., 2006). In order to provide an adequate context, we examined that trait in this study. Consistently, it was found that the chlorophyll content assessed as SPAD index was similar for both genotypes until day 13 AA, being differences between them observed since day 19 AA. On that day and thereafter the SPAD index recorded in the flag leaf was lower in control than in RNAi plants (Figure 1A). It was also observed that maximal photochemical efficiency of photosystem II (Fv/Fm) was similar for both genotypes until day 19 AA, while it became significantly different between lines at day 21 AA, being higher for RNAi than for control plants (Figure 1B). A complementary experiment showed that at a late stage, in agreement with former observations (Uauy et al. 2006; Borrill et al. 2015), senescence in flag leaves also took place in RNAi plants (Supplemental Figure 1).

Another key observation made in the previous study was that the concentration of nitrogen, iron as well as other elements in the flag leaf was lower in control than in RNAi plants (Uauy et al., 2006). Consistent with those findings it was observed here that while both soluble protein and iron concentration in the flag leaf were similar for both genotypes on day 14 AA, they were significantly higher in RNAi than in control plants at day 24 AA (Figure 1C, D). We concluded that control and RNAi plants behave as formerly described, thus providing a solid basis for detailed studies on the processes underlying the stay-green phenotype of RNAi plants. In addition, the polypeptide profile, assessed by SDS-PAGE, was similar at day 14 AA for both lines. On day 24 AA it was observed that RNAi plants maintained high levels of Rubisco per unit of leaf weight compared with control plants, for which both subunits sharply decreased (Fig. 2A).

A first question examined here was the possible relationship between the progression of senescence and the content of carbohydrates. Thus, the concentrations of soluble and non-soluble carbohydrates in the flag leaf were determined in both lines at both harvests. It was observed that control plants displayed a slightly, even non-significant, higher concentration of soluble carbohydrates on day 14 AA than RNAi plants (Figure 3A). On

the other hand both at day 14 AA and day 24 AA, similar values were observed between genotypes in the concentration of non-soluble carbohydrates (Figure 3B). These data indicate that accumulation of total carbohydrates in the flag leaves of control plants was not modified over the period during which both soluble proteins and iron significantly decayed. The possibility that the concentration of major components of the soluble carbohydrates fraction, namely sucrose, glucose and fructose, could differ between lines was also examined. However, both on day 14 AA and on day 24 AA the concentrations of these three compounds were similar for both lines (Figure 3 C, D and E, respectively).

3.2 Changes in quantitative chloroplast parameters explain the early senescence displayed by control plants

Results above suggest a potential connection between the early degradation of chlorophyll, low Fv/Fm, and reduced iron content as well as soluble protein concentrations in the flag leaf of control plants, which could be eventually associated with chloroplast dismantling. In order to test the possibility that chloroplast dismantling occurs earlier in control than in RNAi plants, we isolated flag leaf chloroplasts of both genotypes through standard procedures and examined for changes in their light scattering properties by using a flow cytometer. When both genotypes were compared, it was observed that the forward scatter value, which is associated to organelle size, was similar for control and RNAi plants on day 14 AA and slightly, but not significantly, lower for control plants on day 24 AA (Figure 4A). On the other hand, the side scatter, which can be associated to granularity and complexity (Bortner and Cidlowski, 2007), was similar for both genotypes on day 14 AA but was significantly lower for control than for RNAi plants on day 24 AA (Figure 4B), suggesting that the RNAi genotype preserved chloroplast structure longer. We found that the fluorescence associated with chlorophyll in the chloroplast fraction was sharply reduced on day 24 AA in control but not in RNAi plants, while no differences between lines were observed on day 14 AA (Figure 4C). These results indicate that the stay-green phenotype and the maintenance of parameters associated with photosynthetic performance displayed by RNAi plants are correlated with conservation of chloroplast structure.

3.3 Chloroplasts of RNAi plants do not exhibit early ultrastructural changes

In order to obtain a complementary assessment of the changes undergone by chloroplasts in control and RNAi plants during the period studied here, leaf sections from the middle zone of the flag leaf were obtained and observed with an electron microscope (Figure 5). It was observed that on day 17 AA chloroplasts of both genotypes displayed similar morphological characteristics, being ellipsoidal, showing thylakoid membrane integrity and intact grana stacking. For control plants, on day 24 AA, chloroplasts in that region of the flag leaf were rarely observed. When observed, they typically displayed a transition from ellipsoidal to spherical morphology, reduced grana stacks and increased disruption of thylakoids. On the contrary, in RNAi plants, the number of chloroplasts in that region seemed to be well preserved, while no ultrastructural changes were observed. Therefore, in RNAi plants the lack of visible symptoms of senescence is linked with maintenance of ultrastructural chloroplast integrity.

3.4 Control and RNAi plants exhibit major differences in antioxidant activity

Some *Arabidopsis* NAC transcription factors have been reported to be integrated into the ROS network (Thomas and Oughman, 2014). Therefore, in this work the oxidative damage was evaluated in control and RNAi wheat plants at days 14 and 24 AA through measurement of carbonyl groups in proteins. It was found that protein carbonylation was almost identical for both lines on day 14 AA (Figure 6A). On day 24 AA there was a trend, although not significant, to increased carbonylation in control relative to RNAi plants. Handling ROS is a critical issue since they participate in signalling processes and eventually may lead to oxidative stress conditions. Therefore, some components of the antioxidant response were studied. The redox status of the tissue in terms of glutathione concentration, as estimated by accumulation of thiols, proved to be similar for both lines at both harvests (Figure 6B). In spite of the absence of significant differences in both protein carbonylation and total thiol levels, it was observed that while no differences between genotypes were observed for the activity of SOD and APX on day 14 AA, at day 24 AA

SOD activity, and to a greater extent APX, became sharply reduced in control relative to RNAi plants (Figure 6C and D, respectively, $p<0.05$).

4. Discussion

Pioneering work introduced, ten years ago, the notion that NAC transcription factors are important players in plant senescence (Guo and Gan, 2006; Uauy et al., 2006), being also critical contributors in determining the accumulation of nitrogen, iron and zinc in wheat grains. Establishing RNAi lines with down-regulation of *TaNAM* genes demonstrated that they display a pronounced stay-green phenotype, while having a low content of protein, iron and other nutrients in the grain (Uauy et al., 2006; Waters et al., 2009). The prevalent view is that low delivery of those elements to the grain of these RNAi plants can be attributed, at least partially, to the lack of rapid chloroplast degradation in leaves (Distelfeld et al., 2007; Waters et al., 2009) but no experimental evidence for this hypothesis has been presented so far. Our work provides evidence indicating that while chloroplasts are rapidly dismantled in control plants, maintenance of chlorophyll content in RNAi plants is associated with conservation of chloroplast structural properties and that this correlates with the maintenance of iron and soluble proteins in the flag leaf. In addition our results point out that the flag leaf of these plants also displays a higher functionality of some enzymatic components involved in the antioxidant response.

Results shown here provide support to the idea that the stay-green phenotype displayed by *TaNAM*-RNAi plants is associated with maintenance of chloroplast structure, which was well preserved in these plants within the period under study. Differences in the maintenance of chloroplast ultrastructure, probably through regenerative mechanisms, have been recently shown to play an important role in determining differences in senescence between a wheat stay-green functional variety and a control line (Luo et al., 2013). Evidence obtained here, which includes conservation of chloroplast size, their apparent complexity, thylakoid membrane integrity and intact grana stacking, suggest that preservation of chloroplast ultrastructure is a key component of the stay-green phenotype generated by the down-regulation of *TaNAM* genes. The finding that the attributes mentioned above are not

affected in RNAi plants provides an structural base for the observation made by Avni et al (2014) and more recently by Borrill et al (2015) showing that the stay-green phenotype generated, respectively, by the lack of *TaNAM-A1* and *TaNAM-D1* or RNAi-down regulation of all *TaNAM* genes expression in *T. aestivum* is actually companied by maintenance of photosynthesis. Taken together these data provide support to the idea that lack, or diminished, TaNAM activity generates a functional stay-green phenotype, and that this is accompanied by preservation of full chloroplast structure. Degradation of chloroplasts is considered to be an important source of nitrogen (Martinez et al., 2008; Gregersen et al., 2008), iron (Jeong and Guerinot, 2009) and other nutrients, like zinc (Broadley et al., 2007). In this context, the preservation of chloroplast structure observed here would diminish the pool of nutrients available for export, thus contributing to reduce the export of those nutrients. Besides to the possible differences in nutrient availability derived from differential chloroplast degradation, specific transport processes could be differentially modulated in control plants and those with diminished -or absence of- *NAM* activity as suggested by recent transcriptome studies with *GPC-A1/GPC-B1* mutant plants (Pearce et al., 2014).

Senescence has frequently been reported to be associated with increased production of ROS and the subsequent oxidative damage (Mehta et al., 1992; Hopkins et al., 2007; Krieger-Lizkay et al., 2015). While our results do not show conclusive evidence for increased oxidative damage in control plants and do not suggest major differences in the thiols content of leaves between lines, they indicated that delayed senescence derived from the down-regulation of *TaNAM* genes was associated with a late difference in the enzymatic antioxidant machinery. This suggests that TaNAM factors, as observed for some Arabidopsis NAC transcription factors contribute to set the antioxidant network (Balazadeh et al., 2011; Hickman et al., 2013). Differences in SOD and APX activities between control and RNAi lines observed here were noted when additional symptoms of senescence became self-evident. Therefore, we hypothesized that the contribution of TaNAM to ROS network through modulation of enzymatic activity may be probably related to an indirect effect derived from a global senescence syndrome more than to a primary effect related with ROS signalling, although the last possibility should not be completely discarded. Besides, it should be noted that evidence for a differential control of the antioxidant response in the

tasg1 stay-green *T. aestivum* mutant has been provided (Hui et al., 2012). In this mutant data has been also obtained for preservation of chloroplast ultrastructure (Tian et al., 2012). The important similarities observed between *tasg1* and *NAM-RNAi* plants likely suggest that conservation of chloroplast structure and high enzymatic antioxidant machinery, are common features of different functional stay-green *Triticum aestivum* genotypes. Additional evidence supporting this statement, for the enzymatic antioxidant machinery, has been recently offered for *T. durum* (De Simone et al., 2014). These findings support the view that a convergence of pathways during the execution phase of senescence could take place in wheat as already suggested for *Arabidopsis thaliana* (Guo and Gan, 2012). Besides, our results may have some relevance to interpret the observations made by Guttieri et al. (2013), who found that at high nitrogen supply levels, heat and moisture stresses accelerate the senescence of *TaNAM*-RNAi plants to a lower extent than *TaNAM* plants.

It has been shown that NAM transcription factors act on a specific subset of genes at early stages after anthesis, well before visible symptoms of senescence are observed (Pearce et al., 2014). Our work indicates that, at comparatively early stages of development, no differences in chloroplast ultrastructure seem to exist between control and RNAi plants. The accumulation of soluble carbohydrates has been proposed to be involved in senescence signalling as suggested by detailed studies involving steam-girdling (Parrot et al., 2005; 2007). Although our results do not permit to completely ruling out a differential accumulation of total soluble carbohydrates between control and RNAi plants at an early stage, a possible role of sucrose, glucose or fructose as early differential signalling components in *TaNAM* and *TaNAM*-RNAi plants may not be supported with the present set of data.

In summary results introduced in this work indicate that, within the developmental window studied, chloroplast ultrastructure and enzymatic antioxidant machinery are well preserved in plants with diminished NAM activity, which could provide a functional basis for the low export of nitrogen and iron from the flag leaf.

Contributions

Mariana L. Checovich conducted data obtention, performed the statistical analysis and contributed to data interpretation and manuscript writing. Andrea Galatro and Marcela Simontacchi made carbonylation and thiol determinations, contributed to data analysis, experimental design and manuscript writing. Jorge I. Moriconi made sugar determinations and contributed to data interpretation and manuscript writing. Jorge Dubcovsky revised and edited the manuscript and provided the materials used. Guillermo E. Santa-María designed the experiments, contributed to data interpretation and wrote the manuscript.

Acknowledgements

Thanks are given to Professor Juan José Guiamet (INFIVE, Universidad Nacional de La Plata, Argentina) for critical reading of the manuscript and to Professor Fernando Carrari (Instituto Nacional de Tecnología Agropecuaria, Argentina) for advise with sugar determinations. This work was supported by funds from CONICET and Agencia Nacional de Promoción Científica y Tecnológica (ANPCyT) through PICT 2012/0429 to MS and PICT 2014/1887 to GES-M. MC is fellow from CONICET. Thanks are also given to Patricia Uchiya (Comisión de Investigaciones Científicas, Buenos Aires, Argentina) for valuable technical assistance.

Appendix A. Supplementary data

Supplementary data related to this article can be found in the on-line version.

References

Asplund, L., Bergkvist, G., Leino, M. W., Westerbergh, A., Weih, M. (2013). Swedish spring wheat varieties with the rare high grain protein allele of *NAM-B1* differ in leaf senescence and grain mineral content. PloS one, 8 (3), e59704.

Avni, R., Zhao, R., Pearce, S., Jun, Y., Uauy, C., Tabbita, F., Fahima, T., Slade, A., Dubcovsky, J. Distelfeld, A. (2014). Functional characterization of *GPC-1* genes in hexaploid wheat. Planta, 239 (2), 313-324.

Balazadeh, S., Kwasniewski, M., Caldana, C., Mehrnia, M., Zanor, M. I., Xue, G. P., Mueller-Roeber, B. (2011). ORS1, an H_2O_2-responsive NAC transcription factor, controls senescence in *Arabidopsis thaliana*. Molecular Plant, 4 (2), 346-360.

Borrill, P., Fahy, B., Smith, A. M., Uauy, C. (2015). Wheat grain filling is limited by grain filling capacity rather than the duration of flag leaf photosynthesis: A case study using *NAM* RNAi Plants. PloS one, 10 (8), e0134947.

Bortner, C. D., Cidlowski, J. A. (2007). Cell shrinkage and monovalent cation fluxes: role in apoptosis. Archives of Biochemistry and Biophysics, 462 (2), 176-188.

Bradford, M. M. (1976). A rapid and sensitive method for the quantitation of microgram quantities of protein utilizing the principle of protein-dye binding. Analytical Chemistry 72 (1-2), 248-254.

Brevis, J. C., Dubcovsky, J. (2010). Effects of the chromosome region including the locus on wheat grain and protein yield. Crop Science, 50 (1), 93-104.

Broadley, M.R., White, P.J., Hammond, J.P., Zelko, I., Lux, A. (2007). Zinc in plants. New Phytologist, 173 (4), 677-702.

Cai, S., Yu, G., Chen, X., Huang, Y., Jiang, X., Zhang, G., Jin, X. (2013). Grain protein content variation and its association analysis in barley. BMC Plant Biology, 13 (1), 35.

Cakmak, I., Torun, A., Millet, E., Feldman, M., Fahima, T., Korol, A., Nevo, E., Braun, H.J., Özkan, H. (2004). *Triticum dicoccoides*: an important genetic resource for increasing

zinc and iron concentration in modern cultivated wheat. Soil Science and Plant Nutrition, 50 (7), 1047-1054.

De Simone, V., Soccio, M., Borrelli, G. M., Pastore, D., Trono, D. (2014). Stay-green trait-antioxidant status interrelationship in durum wheat (*Triticum durum*) flag leaf during post-flowering. Journal of Plant Research, 127 (1), 159-171.

Distelfeld, A., Cakmak, I., Peleg, Z., Ozturk, L., Yazici, A. M., Budak, H., Saranga, Y., Fahima, T. (2007). Multiple QTL-effects of wheat *Gpc-B1* locus on grain protein and micronutrient concentrations. Physiologia Plantarum, 129 (3), 635-643.

Distelfeld, A., Korol, A., Dubcovsky, J., Uauy, C., Blake, T., Fahima, T. (2008). Colinearity between the barley grain protein content (GPC) QTL on chromosome arm 6HS and the wheat *Gpc-B1* region. Molecular Breeding, 22 (1), 25-38.

Distelfeld, A., Pearce, S. P., Avni, R., Scherer, B., Uauy, C., Piston, F., Slade, A., Zhao, R., Dubcovsky, J. (2012). Divergent functions of orthologous *NAC* transcription factors in wheat and rice. Plant Molecular Biology, 78 (4-5), 515-524.

Dominguez P.G., Frankel N., Mazuch J., Balblo I., Iusem N., Fernie A.R., Carrari F. (2013). ASR1 mediates glucose-hormone cross talk by affecting sugar trafficking in tobacco plants. Plant Physiology 161 (3), 1486-1500.

Dubois, M., Gilles, K. A., Hamilton, J. K., Rebers, P., Smith, F. (1956). Colorimetric method for determination of sugars and related substances. Analytical Chemistry, 28 (3), 350-356.

Garapati P., Xue G. P., Munné-Bosch S., Balazadeh S. (2015). Transcription factor ATAF1 promotes senescence by direct regulation of key chloroplast maintenance and senescence transcriptional cascades. Plant Physiology 168, 1122-1139.

Gregersen, P. L., Holm, P. B., Krupinska, K. (2008). Leaf senescence and nutrient remobilisation in barley and wheat. Plant Biology, 10 (1), 37-49.

Guttieri M.J., Stein R.J., Waters B.M. (2013). Nutrient partitioning and grain yield of *TaNAM*-RNAi wheat under abiotic stress. Plant and Soil 371, 573-591.

Guo, Y., Gan, S. S. (2012). Convergence and divergence in gene expression profiles induced by leaf senescence and 27 senescence-promoting hormonal, pathological and environmental stress treatments. Plant Cell and Environment 35 (3), 644-655.

Hickman, R., Hill, C., Penfold, C. A., Breeze, E., Bowden, L., Moore, J. D., Zhang, P., Jackson, A., Cooke, E., Bewicke-Copley, F., Mead, A., Beynon, J., Wild, DL., Denby, K. J., Ott, S., Buchanan-Wollaston, V. (2013). A local regulatory network around three *NAC* transcription factors in stress responses and senescence in *Arabidopsis* leaves. The Plant Journal, 75 (1), 26-39.

Hopkins, M., Taylor, C., Liu, Z., Ma, F., McNamara, L., Wang, T. W., Thompson, J. E. (2007). Regulation and execution of molecular disassembly and catabolism during senescence. New Phytologist, 175 (2), 201-214.

Hui, Z., Tian, F. X., Wang, G. K., Wang, G. P., Wang, W. (2012). The antioxidative defense system is involved in the delayed senescence in a wheat mutant *tasg1*. Plant Cell Reports, 31 (6), 1073-1084.

Jamar, C., Loffet, F., Frettinger, P., Ramsay, L., Fauconnier, M. L., Du Jardin, P. (2010). *NAM-1* gene polymorphism and grain protein content in *Hordeum*. Journal of Plant Physiology, 167 (6), 497-501.

Jasid, S., Simontacchi, M., Bartoli, C. G., Puntarulo, S. (2006). Chloroplasts as a nitric oxide cellular source. Effect of reactive nitrogen species on chloroplastic lipids and proteins. Plant Physiology, 142 (3), 1246-1255.

Jeong, J., Guerinot, M. L. (2009). Homing in on iron homeostasis in plants. Trends in Plant Science, 14 (5), 280-285.

Joppa, L. R., Du, C., Hart, G. E., Hareland, G. A. (1997). Mapping gene(s) for grain protein in tetraploid wheat (*Triticum turgidum L.*) using a population of recombinant inbred chromosome lines. Crop Science, 37 (5), 1586-1589.

Jukanti, A. K., Heidlebaugh, N. M., Parrot, D. L., Fischer, I. A., McInnerney, K., Fisher A. M. (2008). Comparative transcriptome profiling of near-isogenic barley (*Hordeum vulgare*) lines differing in the allelic state of a major grain protein content locus identifies genes with possible roles in leaf senescence and nitrogen reallocation. New Phytologist 177, 333-349.

Kade, M., Barneix, A. J., Olmos, S., Dubcovsky, J. (2005). Nitrogen uptake and remobilization in tetraploid 'Langdon' durum wheat and a recombinant substitution line with the high grain protein gene *Gpc-B1*. Plant Breeding, 124 (4), 343-349.

Krieger-Liszkay, A., Trösch, M., Krupinska, K. (2015). Generation of reactive oxygen species in thylakoids from senescing flag leaves of the barley varieties Lomerit and Carina. Planta, 241 (6), 1497-1508.

Levine, R. L., Williams, J. A., Stadtman, E. R., Shacter, E. (1994). Carbonyl assays for determination of oxidatively modified proteins. Methods in Enzymology, (233), 346-357.

Luo, P. G., Deng, K. J., Hu, X. Y., Li, L. Q., Li, X., Chen, J. B., Zhang, H. Y., Tang, Z. X., Zhang, Y., Sun, Q. X., Tan, F. Q., Ren, Z. L. (2013). Chloroplast ultrastructure regeneration with protection of photosystem II is responsible for the functional 'stay-green' trait in wheat. Plant, Cell and Environment, 36 (3), 683-696.

Martínez, D. E., Costa, M. L., Guiamet, J. J. (2008). Senescence-associated degradation of chloroplast proteins inside and outside the organelle. Plant Biology, 10 (s1), 15-22.

Mehta, R. A., Fawcett, T. W., Porath, D., Mattoo, A. K. (1992). Oxidative stress causes rapid membrane translocation and in vivo degradation of ribulose-1, 5-bisphosphate carboxylase/oxygenase. Journal of Biological Chemistry, 267 (4), 2810-2816.

Moriconi, J. I., Buet, A., Simontacchi, M., Santa-María, G. E. (2012). Near-isogenic wheat lines carrying altered function alleles of the *Rht-1* genes exhibit differential responses to potassium deprivation. Plant Science, 185-186, 199-207.

Parrott, D., Yang, L., Shama, L., Fischer, A. M. (2005). Senescence is accelerated, and several proteases are induced by carbon "feast" conditions in barley (*Hordeum vulgare L.*) leaves. Planta, 222 (6), 989-1000.

Parrott, D. L., McInnerney, K., Feller, U., Fischer, A. M. (2007). Steam-girdling of barley (*Hordeum vulgare*) leaves leads to carbohydrate accumulation and accelerated leaf senescence, facilitating transcriptomic analysis of senescence-associated genes. New Phytologist, 176 (1), 56-69.

Pearce, S., Tabbita, F., Cantu, D., Buffalo, V., Avni, R., Vazquez-Gross, H., Zhao, R., Conley, J. C., Distelfeld, A., Dubcovksy, J. (2014). Regulation of Zn and Fe transporters by the *GPC1* gene during early wheat monocarpic senescence. BMC Plant Biology, 14 (1), 368.

Prochazkova, D., Sairam, R. K., Srivastava, G. C., Singh, D. V. (2001). Oxidative stress and antioxidant activity as the basis of senescence in maize leaves. Plant Science, 161, 765-771.

Sies, H., Akerboom, T. P. (1984). Glutathione disulfide (GSSG) efflux from cells and tissues. Methods in Enzymology, 105, 445-451.

Tabbita, F., Lewis, S., Vouilloz, J. P., Ortega, M. A., Kade, M., Abbate, P. E., Barneix, A. J. (2013). Effects of the *Gpc-B1* locus on high grain protein content introgressed into Argentinean wheat germplasm. Plant Breeding, 132 (1), 48-52.

Thomas, H., Howarth, C. J. (2000). Five ways to stay green. Journal of Experimental Botany, 51 (1), 329-337.

Thomas, H., Ougham, H. (2014). The stay-green trait. Journal of Experimental Botany, 65 (14), 3889-3900.

Thompson, J. E., Legge, R. L., Barber, R. F. (1987). The role of free radicals in senescence and wounding. New Phytologist, 105 (3), 317-344.

Tian, F. X., Gong, J. F., Wang, G. P., Wang, G. K., Fan, Z. Y., Wang, W. (2012). Improved drought resistance in a wheat stay-green mutant tasg1 under field conditions. Biologia Plantarum, 56 (3), 509-515.

Uauy, C., Distelfeld, A., Fahima, T., Blechl, A., Dubcovsky, J. (2006). A NAC gene regulating senescence improves grain protein, zinc, and iron content in wheat. Science, 314 (5803), 1298-1301.

Waters, B. M., Uauy, C., Dubcovsky, J., Grusak, M. A. (2009). Wheat *(Triticum aestivum)* NAM proteins regulate the translocation of iron, zinc, and nitrogen compounds from vegetative tissues to grain. Journal of Experimental Botany, 60 (15), 4263-4274.

Figure legends

Figure 1. Chlorophyll content, maximal photochemical efficiency of photosystem II, concentration of soluble proteins and iron in control and *TaNAM*-RNAi plants as determined in the flag leaf within the first 24 DAA. A, clorophyll content as determined

from the SPAD index; B, maximal photochemical efficiency of photosystem II (Fv/Fm). C, content of soluble proteins expressed on a fresh weight basis; D, content of iron expressed on a dry weight basis. In A and B data are the mean of 20 independent replicates $\pm$ SE. In C and D data are the mean of 5 and 15 independent replicates, respectively. Bars correspond to SE. One asterisk denotes significant differences between genotypes at $p<0.05$, two asterisks denote significant differences at $p<0.01$ and three asterisks significant differences at $p<0.001$ (t-test).

Figure 2. A, SDS-PAGE of control and *TaNAM*-RNAi leaves at 14 and 24 DAA. In each lane, soluble protein extracts corresponding to 6.5 mg of fresh tissue were loaded. Lane 1: Control 14 DAA, Lane 2: RNAi 14 DAA, Lane 3: Control 24 DAA, Lane 4: RNAi 24 DAA. The molecular weight corresponding to the large (LS) and small (SS) Rubisco subunits is indicated.

Figure 3. Concentration of soluble and non-soluble carbohydrates in flag leaves of control and *TaNAM*-RNAi plants at 14 and 24 DAA. A, soluble carbohydrates; B, non-soluble carbohydrates; C, sucrose; D, glucose and E, fructose, respectively. Concentrations are expressed on a fresh weight basis. Data correspond to the mean value of 5 independent replicates, bars indicate SE.

Figure 4. Properties of chloroplasts extracted from flag leaves of control and *TaNAM*-RNAi plants at 14 and 24 DAA. A, forward scatter value, associated with organelle size; B, side scatter, associated to granularity and complexity; C, chlorophyll fluorescence. Data correspond to the mean of four independent replicates with SE. One asterisk denotes significant differences between genotypes at $p<0.05$ and three asterisks significant differences at $p<0.001$ (t-test). Values correspond to arbitrary units.

Figure 5. Transmission electron microscopy photographs of control and *TaNAM*-RNAi plants before (17 DAA) and once differences in SPAD index between genotypes were

observed (24 DAA). Representative pictures obtained from A, control plants (17 DAA); B, RNAi plants (17 DAA); C, control plants (24 DAA); D, RNAi plants (24 DAA). Note differences in the scale.

Figure 6. Oxidative damage, thiol content and enzymatic antioxidant activity in control and *TaNAM*-RNAi plants at 14 and 24 DAA. A, protein carbonylation expressed per unit of protein; B, C, and D, thiol content, SOD activity and APX activity expressed per unit of fresh weight, respectively. Data correspond to the mean of five independent replicates with SE. The asterisk denotes significant differences between genotypes at $p<0.05$ (t-test).

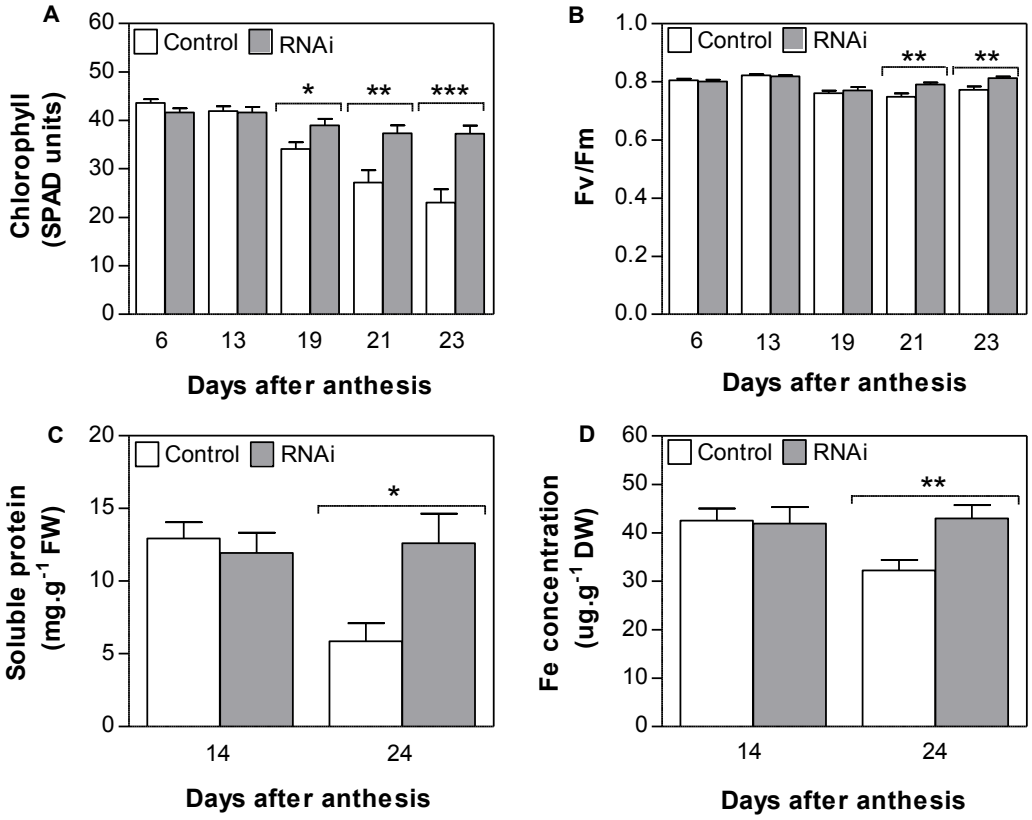

Figure 1. Chlorophyll content, maximal photochemical efficiency of photosystem II, concentration of soluble proteins and iron in control and *TaNAM*-RNAi plants as determined in the flag leaf within the first 24 DAA. A, clorophyll content as determined from the SPAD index; B, maximal photochemical efficiency of photosystem II (Fv/Fm). C, content of soluble proteins expressed on a fresh weight basis; D, content of iron expressed on a dry weight basis. In A and B data are the mean of 20 independent replicates $\pm$ SE. In C and D data are the mean of 5 and 15 independent replicates, respectively. Bars correspond to SE. One asterisk denotes significant differences between genotypes at $p<0.05$, two asterisks denote significant differences at $p<0.01$ and three asterisks significant differences at $p<0.001$ (t-test).

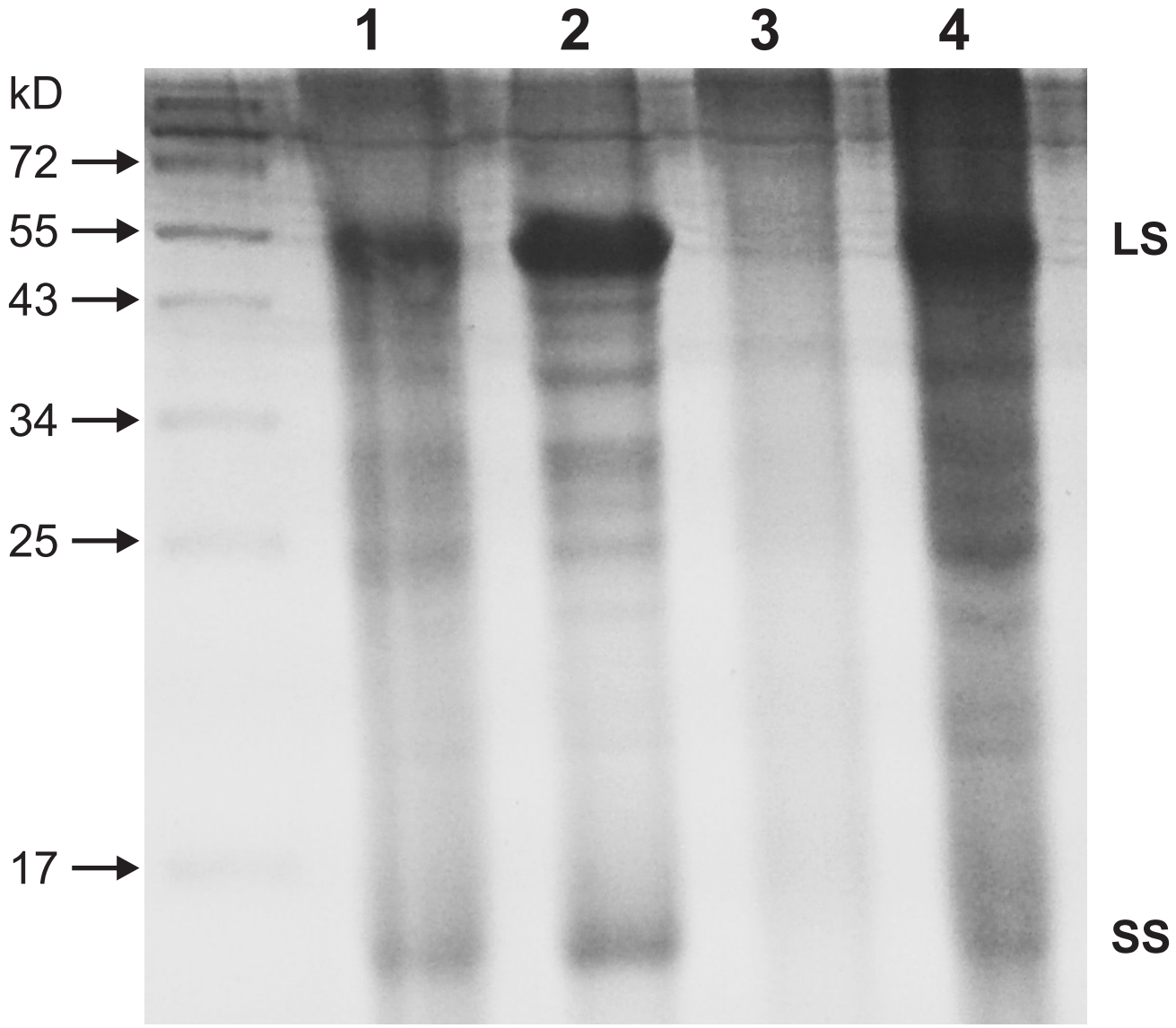

Figure 2. A, SDS-PAGE of control and TaNAM-RNAi leaves at 14 and 24 DAA. In each lane, soluble protein extracts corresponding to 6.5 mg of fresh tissue were loaded. Lane 1: Control 14 DAA, Lane 2: RNAi 14 DAA, Lane 3: Control 24 DAA, Lane 4: RNAi 24 DAA. The molecular weight corresponding to the large (LS) and small (SS) Rubisco subunits is indicated.

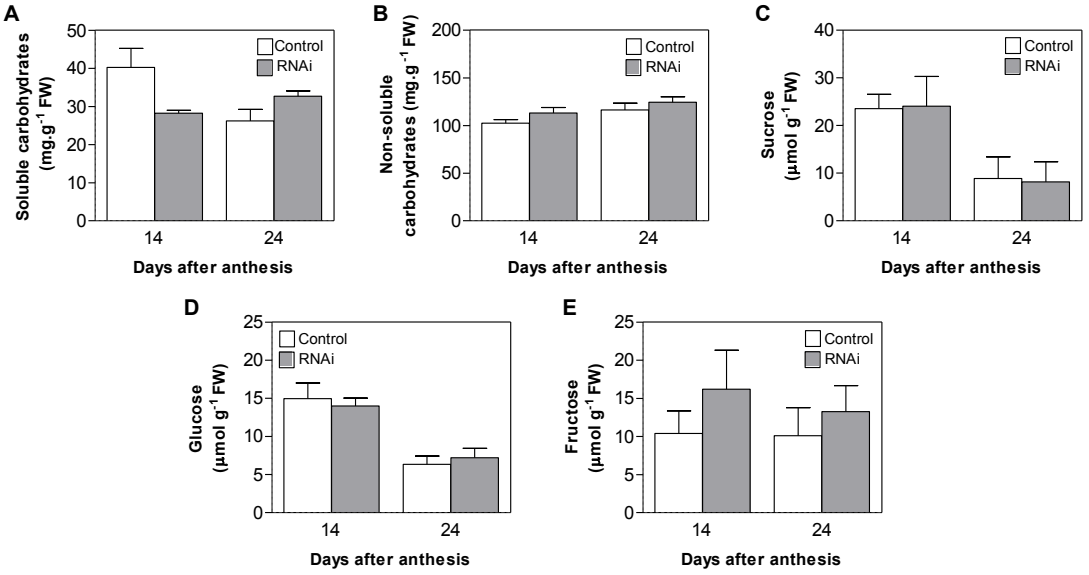

Figure 3. Concentration of soluble and non-soluble carbohydrates in flag leaves of control and *TaNAM*-RNAi plants at 14 and 24 DAA. A, soluble carbohydrates; B, non-soluble carbohydrates. In C, D and E, the concentrations of sucrose, glucose and fructose, expressed on a fresh weight basis are shown, respectively. Data correspond to the mean value of 5 independent replicates, bars indicate SE.

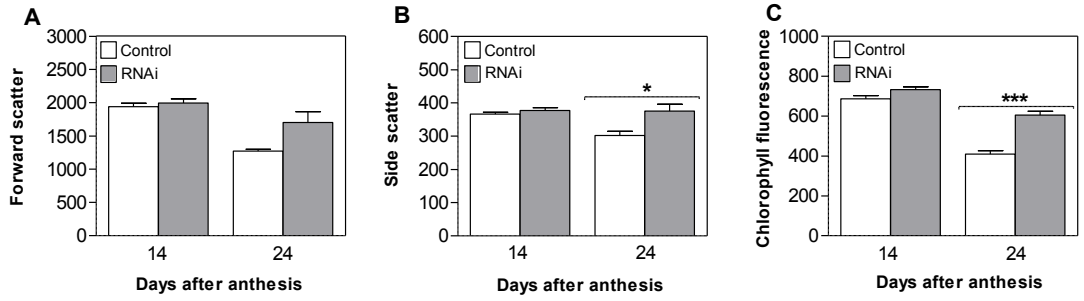

Figure 4. Properties of chloroplasts extracted from flag leaves of control and *TaNAM*-RNAi plants at 14 and 24 DAA. A, forward scatter value, associated with organelle size; B, side scatter, associated to granularity and complexity; C, chlorophyll fluorescence. Data correspond to the mean of four independent replicates with SE. One asterisk denotes significant differences between genotypes at $p<0.05$ and three asterisks significant differences at $p<0.001$ (t-test). Values correspond to arbitrary units.

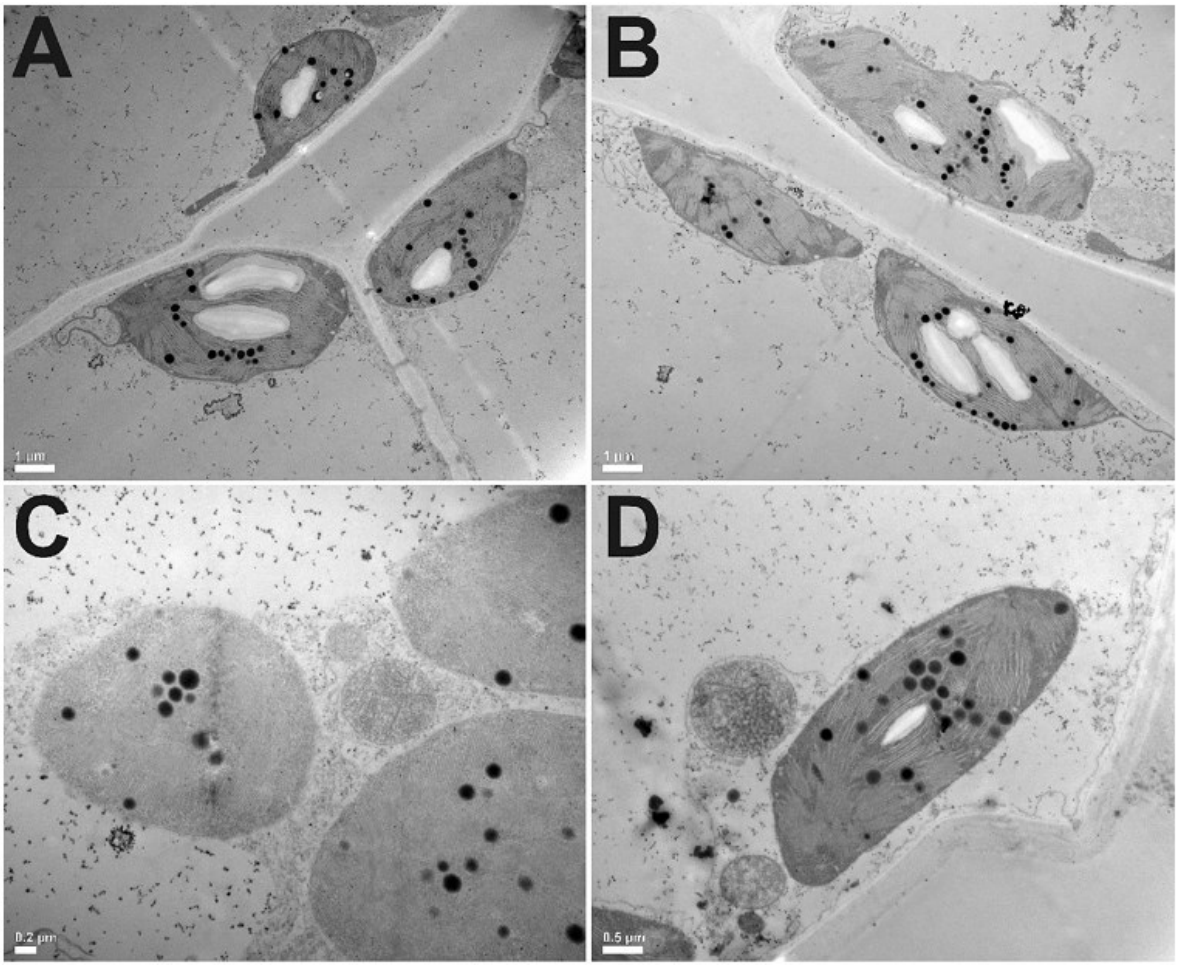

Figure 5. Transmission electron microscopy photographs of control and *TaNAM*-RNAi plants before (17 DAA) and once differences in SPAD index between genotypes were observed (24 DAA). Representative pictures obtained from A, control plants (17 DAA); B, RNAi plants (17 DAA); C, control plants (24 DAA); D, RNAi plants (24 DAA). Note differences in the scale.

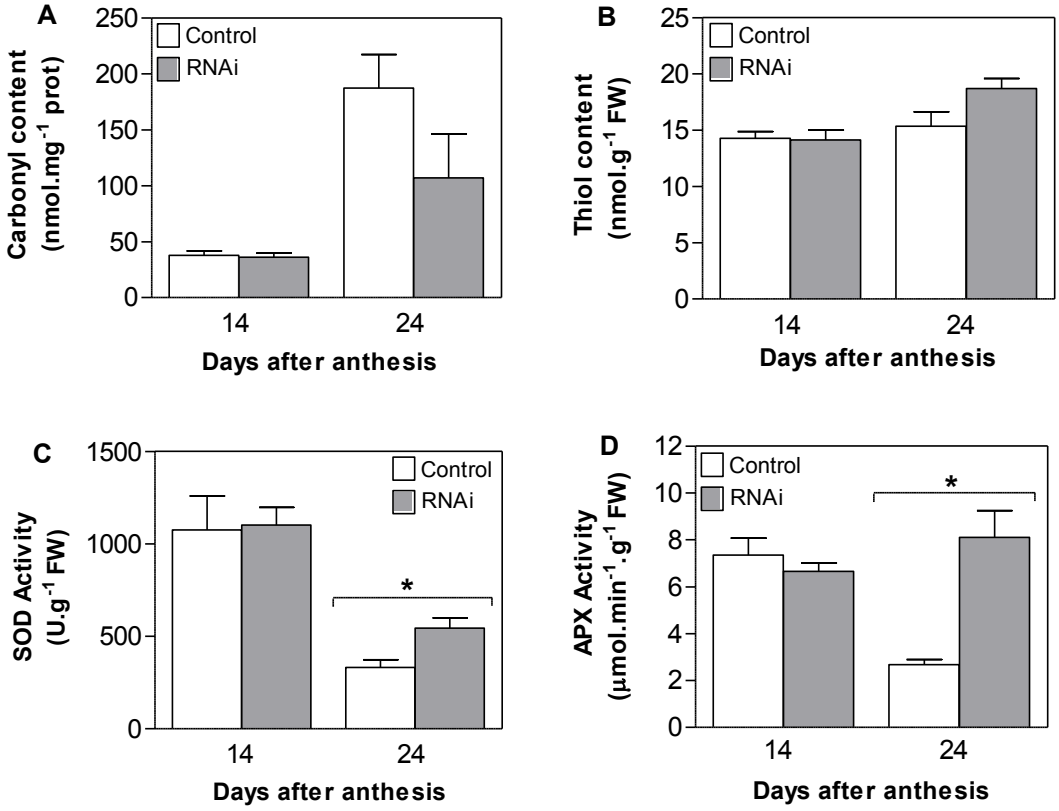

Figure 6. Oxidative damage, thiol content and enzymatic antioxidant activity in control and *TaNAM*-RNAi plants at 14 and 24 DAA. A, protein carbonylation expressed per unit of protein; B, C, and D, thiol content, SOD activity and APX activity expressed per unit of fresh weight, respectively. Data correspond to the mean of five independent replicates with SE. The asterisk denotes significant differences between genotypes at $p<0.05$ (t-test).

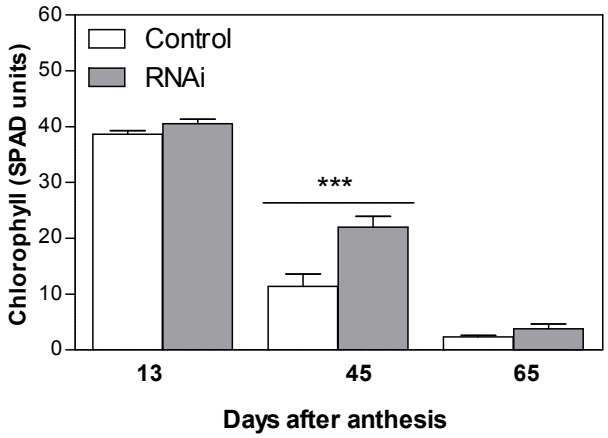

Supplemental Figure 1. Decay of SPAD index also takes place in the flag leaf of *TaNAM*-RNAi plants at a late stage. Data correspond to a separate experiment started on March 13th, 2013. Data are the mean of nine replicates. Bars indicate SE. The three asterisks denote significant differences at $p<0.001$ (t-test).